ALIGN/FOCUS: Laboratory End-to-End Terminal Demonstration and BER Performance Characterisation

Amna Riaz, Eamon Scullion, Robert T. Wicks, Richard Binns, Jethro Vernon, Elías Obreque-Sepúlveda, Nassima Khorchef, James Martin
School of Engineering, Physics and Mathematics, Northumbria University, Newcastle upon Tyne, UK
amna.riaz@northumbria.ac.uk

***Abstract*—Free-space optical communication (FSOC) offers higher data rates than RF while remaining compatible with the strict size, weight, and power (SWaP) constraints of CubeSat platforms. Despite this potential, establishing reliable CubeSat-class optical terminals is non-trivial: link performance is highly sensitive to pointing and alignment, onboard power and thermal margins are limited, and repeatable integration and test procedures are required before flight. This paper presents a laboratory end-to-end demonstration and systematic performance characterisation of the ALIGN/FOCUS CubeSat-scale optical terminal operating at 1550 nm. Terminal performance is characterised over an indoor free-space path by measuring BER as a function of received optical power and amplifier operating conditions. The terminal supports 1.25 Gb/s NRZ-OOK transmission and achieves unamplified BER of 5.73×10^{-7} and amplified BER $< 10^{-9}$ in high-power mode under controlled laboratory conditions. Robustness to pointing misalignment is also characterised, including closed-loop recovery behaviour. Together, these results establish a laboratory-validated system baseline and de-risk the transition toward outdoor and in-orbit demonstration.**

***Index Terms*—CubeSat, free-space optical communication, FSOC, bit error rate, NRZ-OOK, optical amplifier, optical inter-satellite link, ALIGN, FOCUS, indoor testbed.**

I. Introduction

Optical inter-satellite links (OISLs) offer licence-free gigabit-class data rates within the SWaP constraints of 6U CubeSat platforms, positioning them as a key enabler for high-throughput LEO constellations [1], [2]. As Earth-observation and science payloads generate ever larger data volumes, the ability to close a 1 Gb/s-class link at inter-satellite ranges has become a programme-enabling requirement [3], [4].

Most published studies report either in-orbit link demonstrations or component-level laboratory testing of individual subsystems [3], [5], [6]. End-to-end laboratory BER measurements across a real free-space path, using the actual terminal modules, are less commonly reported [7], [8]. Building on prior subsystem-level AWG characterisation of the FOCUS terminal [9], this work extends validation to an indoor free-space terminal demonstration, including BER characterisation versus amplifier operating point and pointing misalignment. Section II describes the terminal and testbed. Section III describes the experimental methods. Section IV presents all results.

TABLE I
ALIGN/FOCUS Key Terminal Parameters

Parameter	Value
Data wavelength	1550 nm, NRZ-OOK
Beacon wavelength	976 nm
Line rate	1.25 Gb/s
Unamplified Tx power	up to ∼6.5 mW
Amplified Tx power	up to ∼425 mW
Amplifier power draw	<23 W (85–92% eff.)
Beacon output	∼0.33 W @ 540 mA
Receiver	Avalanche photodiode (APD)
Tx beam quality	M^2≈1.09, ∼220 µrad

II. FOCUS Terminal

The FOCUS (Free-space Optical Communications Unit for Satellites) terminal is a 3U, < 3 kg, < 15 W payload carried by two identical 6U CubeSats in SSO at 567 km. It operates at 1.25 Gb/s NRZ-OOK at 1550 nm with an onboard optical amplifier, and uses a 976 nm beacon and closed-loop FSM/PSD for pointing, acquisition, and tracking (PAT) [10], [11]. The full module architecture and end-to-end signal flow are shown in Fig. 1(c); key terminal parameters are listed in Table I.

III. Experimental Methods

The indoor free-space testbed consists of a single optical bench housing both the Tx and Rx terminal modules, as shown in Figs. 1(a) and 1(b). The Tx side comprises the data laser, beacon laser, and collimated free-space combiner, which co-boresights the 1550 nm data beam and 976 nm beacon onto a common optical axis, replicating the dual-wavelength flight geometry. The Rx side comprises the focusing lens, 1.5 mm aperture mask, and the PSD-APD detector stack. Calibrated optical attenuators of different attenuation levels are inserted in the path to emulate free-space link loss and set received power during BER sweeps.

The signal chain for BER characterisation is as follows. A Keysight M8190A arbitrary waveform generator (AWG) produces a 1.25 Gb/s NRZ-OOK PRBS-7 pattern that modulates the 1550 nm data laser. The transmitted optical beam propagates across the free-space path and is incident on the APD receiver

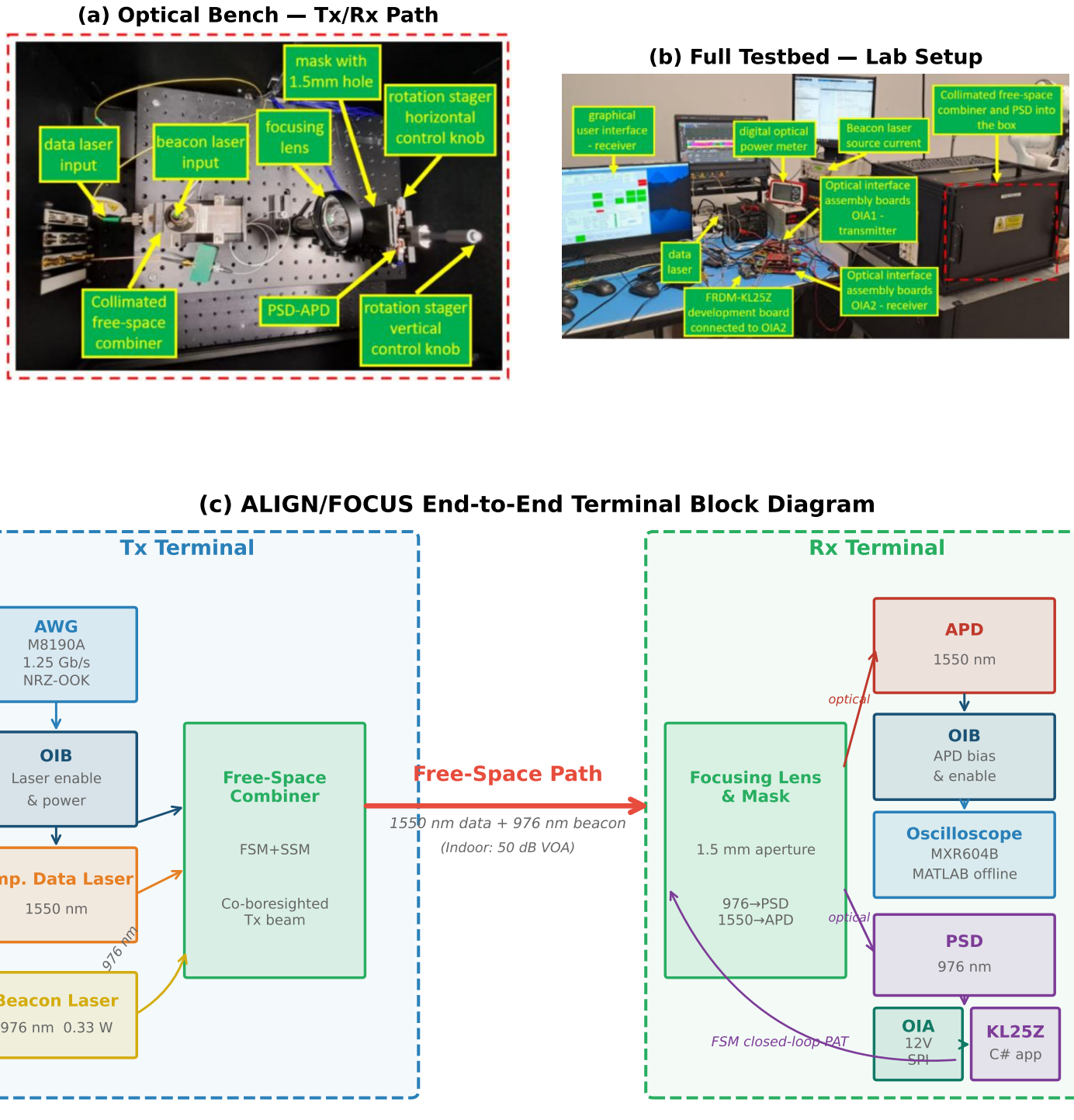

Fig. 1. ALIGN/FOCUS indoor free-space testbed. (a) Optical bench showing the collimated free-space combiner, data and beacon laser inputs, focusing lens, 1.5 mm aperture mask, and PSD-APD detector stack. (b) Full laboratory setup showing OIA boards, KL25Z readout board, data laser, optical power meter, and free-space combiner enclosure. (c) End-to-end block diagram: Tx terminal (AWG modulates Amp. Data Laser; OIB provides laser power and enable; Free-Space Combiner co-boresights 1550 nm and 976 nm beams) and Rx terminal (Focusing Lens and Mask split received beam: 1550 nm to APD data path, OIB biases APD, oscilloscope captures signal for MATLAB offline BER; 976 nm to PSD PAT path, OIA interfaces PSD, KL25Z closes FSM loop).

on the opposite bench, which converts the received optical signal to an electrical signal. The OIB sets the APD bias voltage to characterise sensitivity versus multiplication gain. The resulting electrical signal is captured on a Keysight MXR604B oscilloscope (6 GHz, 16 GSa/s), synchronised to the AWG, and processed offline in MATLAB for eye-diagram capture and BER extraction. Received optical power is measured using a calibrated Thorlabs S144C thermal power sensor ($\pm 3\%$ accuracy). Each measurement is repeated three times under the same laboratory conditions, yielding standard deviations below 3%.

Alignment is performed hierarchically in two stages. At the component level, each optical element — fibre collimator, combiner, FSM, PSD, and receive optics — is fixed to datum references on the optical bench. At the system level, alignment is closed iteratively: the 976 nm beacon is centred on the PSD, the FSM null is commanded, and the 1550 nm data beam is co-boresighted onto the receive aperture using APD photocurrent maximisation. PSD position readbacks are logged through an FSM look-up table, and a hysteresis calibration is stored as a machine-readable artefact to ensure run-to-run reproducibility.

The PSD output is routed via the OIA board, which provides 12 V power and the analogue interface to the PSD/APD stack. The KL25Z microcontroller board connects to the OIA via SPI and reads PSD position values at 6 kHz. Position estimates are computed from the XSUM, XDIFF, YSUM, YDIFF signals of the PSD, with 5,000 samples collected per 80 ms burst.

BER sweeps are conducted in two configurations: unamplified (seed laser routed directly through a calibrated optical attenuator to the APD) and amplified (seed laser via onboard optical amplifier, combiner, and free-space path to APD). Received power is varied by switching between calibrated optical attenuators of different attenuation levels; BER is extracted from the oscilloscope eye diagram at each level. A back-to-back optical baseline is recorded before every session to confirm the measurement chain is nominal.

Controlled misalignment is introduced by commanding incremental angular offsets to the transmitting FSM while the receiving terminal runs the closed-loop PSD–FSM tracking algorithm. Link metrics — received optical power, APD photocurrent, eye opening, and BER — are recorded as a function of pointing offset. The simulated jitter profile used for closed-loop testing follows the EnduroSat ADCS attitude-error envelope ($\pm 1^\circ$ pitch and yaw) [10].

IV. Results and Discussion

A sine-wave sweep confirmed the receive-chain -3 dB bandwidth at 750 MHz, providing adequate analogue bandwidth for 1.25 Gb/s NRZ-OOK operation. The optical amplifier reaches thermal equilibrium with stable beam properties across its full operating range [12], [13], confirming thermal lensing is not a limiting factor.

Fig. 2 shows measured BER as a function of received optical power at 1.25 Gb/s (APD 60 V) for unamplified and amplified configurations. In the unamplified configuration, the terminal achieves BER $= 5.73 \times 10^{-7}$ at 1.25 Gb/s —

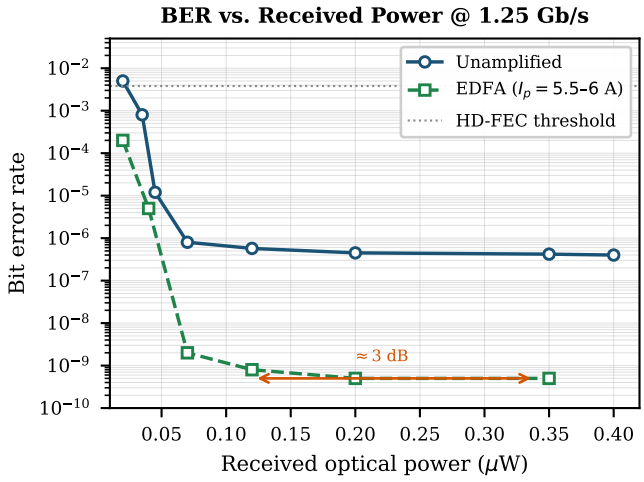

Fig. 2. Measured BER vs. received power at 1.25 Gb/s, APD 60 V, for unamplified and amplified (high-power mode) configurations. Amplified mode shifts the BER threshold by ≈3 dB relative to unamplified operation, yielding BER $< 10^{-9}$ at 0.12 µW.

well below the hard-decision FEC threshold (3.8×10^{-3}). Engaging the optical amplifier in high-power mode When the optical amplifier is operated in high-power mode, the receiver sensitivity improves by approximately 3 dB. This reduces BER to below 10^{-9} at a received power of 0.12 µW, which corresponds to approximately $1.4\times$ extension in link range at the same BER [14]. Eye diagrams show increased signal amplitude and reduced timing jitter compared to the unamplified case.

Fig. 3 shows how BER changes with the amplifier drive setting at 50 dB attenuation for APD bias voltages of 40 V and 60 V. At low drive settings, BER stays in the 10^{-4}–10^{-3} range, which is within the FEC-correctable region. At high drive settings, BER drops below 10^{-9} for all tested APD voltages. The peak amplified output of 0.22 W is achieved at a bus power of 23 W, which is within the power budget of a deployable 6U CubeSat. This gives mission operators the flexibility to trade amplifier power consumption against link reliability on a pass-by-pass basis. The next section examines how well this performance holds under pointing misalignment.

Angular misalignments are introduced per the protocol in Section III. BER degrades monotonically with pointing offset, tracking the expected Gaussian coupling-loss profile for the 220 µrad transmit divergence. Within the FSM dynamic range ($\pm 1^\circ$), the closed-loop servo recovers beam centroids to within 0.04° on sub-second timescales after each offset event, returning the link to nominal BER without manual intervention [10], [15], [16]. Beyond the FSM dynamic range, BER exceeds the FEC threshold and a new spiral acquisition is required. This establishes two operationally critical bounds for mission link-budget planning: the pointing loss coefficient (coupling loss per unit angular offset) and the re-acquisition threshold.

Outdoor propagation effects (atmospheric scintillation,

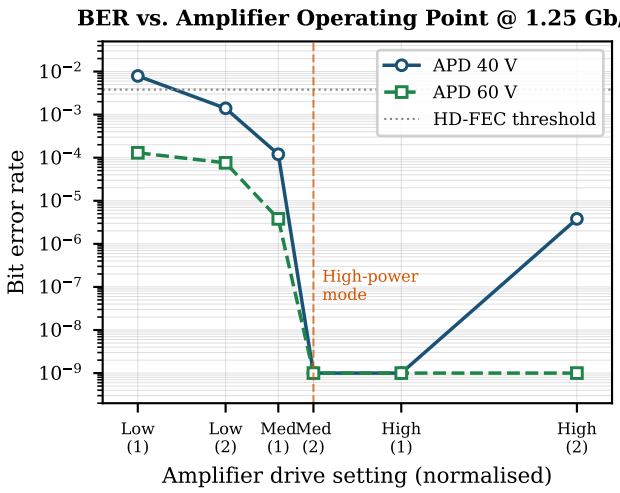

Fig. 3. BER vs. amplifier operating point at 1.25 Gb/s (50 dB attenuation) for APD bias 40 V and 60 V. High-power mode yields BER $< 10^{-9}$; low-power mode remains FEC-correctable, enabling pass-by-pass power–performance trade-offs.

Doppler shift, relative-motion beam wander) are outside the scope of this indoor campaign and will be characterised in follow-on field trials.

V. Conclusion

This paper has presented an integrated laboratory demonstration and systematic performance characterisation of the ALIGN/FOCUS CubeSat-scale optical terminal at 1.25 Gb/s, 1550 nm. The terminal achieves unamplified BER 5.73×10^{-7}, and amplified BER $< 10^{-9}$ in high-power mode — representing ≈ 3 dB sensitivity gain and $\approx 1.4\times$ link-range extension. Robustness to pointing error is confirmed with sub-second closed-loop FSM recovery within the $\pm 1^{\circ}$ dynamic range. Together, these results establish a laboratory-validated system baseline and de-risk the transition toward outdoor and in-orbit demonstration on the ALIGN mission.

Acknowledgment

This research was funded by the UK Space Agency (UKSA) via the National Space Innovation Programme (NSIP), grant UK-SAG22 0042, for Phase 3 of the project titled “ALIGN Laser Optical Communications for CubeSats.” The authors would like to pay special thanks to project partners Telespazio UK Ltd, CfAI Durham University, and SMS Electronics Ltd for continued support throughout the project period.

References

[1] H. Kaushal and G. Kaddoum, “Optical communication in space: Challenges and mitigation techniques,” *IEEE Commun. Surveys Tuts.*, vol. 19, no. 1, pp. 57–96, 2017.

[2] M. Toyoshima, “Recent trends in space laser communications for small satellites and constellations,” *J. Lightwave Technol.*, vol. 39, no. 3, pp. 693–699, Feb. 2021.

[3] D. R. Kolev *et al.*, “Latest developments in the field of optical communications for small satellites and beyond,” *J. Lightwave Technol.*, vol. 41, no. 12, pp. 3750–3757, 2023.

[4] C. M. Schieler *et al.*, “On-orbit demonstration of 200-Gbps laser communication downlink from the TBIRD CubeSat,” in *Proc. SPIE Free-Space Laser Commun. XXXV*, vol. 12413, p. 1241302, 2023.

[5] R. Rüddenklau *et al.*, “In-orbit demonstration of acquisition and tracking on OSIRIS4CubeSat,” *Opt. Express*, vol. 32, no. 23, pp. 41188–41200, 2024.

[6] O. Čierny *et al.*, “Testing of the CubeSat Laser Infrared CrosslinK (CLICK-A) payload,” in *Proc. 34th Annu. AIAA/USU Conf. Small Satellites*, paper SSC20-WKIII-03, 2020.

[7] J. R. Nonay *et al.*, “Horizontal free-space optical link with CubeISL over 143 km,” *J. Opt. Commun. Netw.*, vol. 16, no. 5, pp. 593–601, 2024.

[8] C. Roubal *et al.*, “Laser terminals on CubeSats: Developments for telecommunications and quantum links,” *Int. J. Satell. Commun. Netw.*, vol. 43, no. 3, pp. 133–146, 2025.

[9] A. Riaz *et al.*, “ALIGN: 1 Gbps Optical Inter-Satellite Link Demonstration on 6U CubeSats with the FOCUS Terminal,´´ accepted for presentation at *IEEE Int. Conf. Communications (ICC)*, 2026.

[10] R. Zia-Ul-Mustafa *et al.*, “Pointing, acquisition, and tracking (PAT) for optical satellite communications: Recent trends and the ALIGN UK mission’s PAT mechanism,” in *Proc. IEEE Int. Conf. Space Optical Systems and Applications (ICSOS)*, 2025, pp. 1–10.

[11] Y. Kaymak *et al.*, “A survey on acquisition, tracking, and pointing mechanisms for mobile free-space optical communications,” *IEEE Commun. Surveys Tuts.*, vol. 20, no. 2, pp. 1104–1123, 2018.

[12] A. Riaz *et al.*, “Characterisation of amplified laser beam profiles subject to changing EDFA pump currents in CubeSats,” in *Free-Space Laser Communications XXXVII*, vol. 13355, pp. 457–462, SPIE, 2025.

[13] A. Carrasco-Casado *et al.*, “Development and space-qualification of a miniaturized CubeSat’s 2-W EDFA for space laser communications,” *Electronics*, vol. 11, no. 15, p. 2468, 2022.

[14] A. Carrasco-Casado *et al.*, “Miniaturized multi-platform free-space laser-communication terminals for beyond-5G networks and space applications,” *Photonics*, vol. 11, no. 6, p. 545, 2024.

[15] C. Graham *et al.*, “Steering mirror system with closed-loop feedback for free-space optical communication terminals,” *Aerospace*, vol. 11, no. 5, p. 330, 2024.

[16] P. Grenfell *et al.*, “Pointing, acquisition, and tracking for small satellite laser communications,” in *Proc. 32nd Annu. AIAA/USU Conf. Small Satellites*, paper SSC18-WKI-06, Aug. 2018.